Atmos. Chem. Phys. Discuss., https://doi.org/10.5194/acp-2018-1366
Manuscript under review for journal Atmos. Chem. Phys.
Discussion started: 15 February 2019

Atmospheric Chemistry and Physics Discussions

Influence of functional groups on toxicity of carbon nanomaterials: implication for toxicological evolution during atmospheric relevant aging of soot

Yongchun Liu [1, 2], Haotian Jiang [2, 4], Chunmei Liu [3], Yanli Ge [2], Lian Wang [2], Bo Zhang [2], Hong He [2, 4,5], Sijin Liu [2, 4]

[1] Aerosol and Haze Laboratory, Advanced Innovation Center for Soft Matter Science and Engineering, Beijing University of Chemical Technology, Beijing, 100029, China

[2] State Key Joint Laboratory of Environment Simulation and Pollution Control, Research Center for Eco-Environmental Sciences, Chinese Academy of Sciences, Beijing, 100085, China

[3] Bioduro Technology (Beijing) Co., Ltd., Beijing, 102200, China

[4] University of Chinese Academy of Sciences, Beijing, 100049, China

[5] Center for Excellence in Urban Atmospheric Environment, Institute of Urban Environment, Chinese Academy of Sciences, Xiamen 361021, China.

Correspondence to: Y. Liu (liuyc@buct.edu.cn) and S. Liu (sjliu@rcees.ac.cn)

Abstract:

It has been well recognized that carbon nanomaterials and soot particles are toxic for human health, while it is still controversial about the influence of functionalization on their toxicity as well as the evolution of the toxicity of carbon nanomaterials due to chemical aging in the atmosphere. In the current study, the oxidation potential measured by dithiothreitol (DTT) decay rate and the cytotoxicity to murine macrophage cells of different functionalized carbon nanomaterials were investigated for understanding the role of functionalization in their toxicities. The DTT decay rates of special black 4A

Atmos. Chem. Phys. Discuss., https://doi.org/10.5194/acp-2018-1366
Manuscript under review for journal Atmos. Chem. Phys.
Discussion started: 15 February 2019

Atmospheric Chemistry and Physics Discussions

(SB4A), graphene, graphene oxide, single wall carbon nanotubes (SWCNT), SWCNT-OH and SWCNT-COOH were 45.9±3.0, 58.5±6.6, 160.7±21.7, 38.9±8.9, 57.0±7.2 and 36.7±0.2 pmol $min^{-1}\mu g^{-1}$, respectively. Epoxide was found to be mainly responsible for the largest DTT decay rate of graphene oxide compared with other carbon nanomaterials based on comprehensive characterizations. Both carboxylation and hydroxylation showed little influence on the oxidation potential of carbon nanomaterials, while epoxidation contributes to the enhancement of oxidation potential. All these carbon nanomaterials were toxic to murine J774 cell line. However, oxidized carbon nanomaterials (graphene oxide, SWCNT-OH and SWCNT-COOH) showed weaker cytotoxicity to J774 cell line compared with the corresponding control sample as far as the metabolic activity was considered and stronger cytotoxicity to J774 cell line regarding to the membrane integrity and DNA incorporation. These results imply that epoxidation might enhance the oxidation potential of soot particles during transport.

Atmos. Chem. Phys. Discuss., https://doi.org/10.5194/acp-2018-1366
Manuscript under review for journal Atmos. Chem. Phys.
Discussion started: 15 February 2019

Introduction

Soot, which originates from incomplete combustion, is a mixture of elemental carbon and organic carbon (OC) compounds (Muckenhuber and Grothe, 2006). The adverse effect of soot particles on human health has attracted much attention in the atmospheric chemistry community (Baumgartner et al., 2014). For example, mitochondrial damage in alveolar macrophages and bronchial epithelial cells resulted from exposure of diesel exhaust particles (DEPs) has been observed (Li et al., 2002a;Li et al., 2002b). Oxidation stress or reactive oxygen generation (ROS) is one of mechanisms related to the toxicity of particles including soot particles (Nel et al., 2006), and has been even used as a paradigm to assess particle toxicity (Xia et al., 2006).

Dithiothreitol (DTT) decay rate is commonly used as a cell-free measure of the oxidative potential of different particles (Cho et al., 2005;Charrier and Anastasio, 2012;Kumagai et al., 2002), such as ambient particles (Li et al., 2003;Fang et al., 2016;Cho et al., 2005;Charrier and Anastasio, 2012;Wang et al., 2013), secondary organic aerosol (SOA) (McWhinney et al., 2013b), DEP (Li et al., 2009;McWhinney et al., 2013a), carbon nanotubes (CNT)(Liu et al., 2015), flame soot (Antinolo et al., 2015;Holder et al., 2012;Li et al., 2013) and commercial carbon black (CB) particles (Koike and Kobayashi, 2006;Li et al., 2009;Li et al., 2015;Li et al., 2013). However, the reported DTT decay rate of soot and CB particles varied substantially, from 0.9 to ~50 pmol min^{-1} μg^{-1}. The variation of DTT decay rate among different samples implies the importance of the composition or structure of particles in their toxicities.

Although transition metals, element carbon, humic-like substances and quinones

Atmos. Chem. Phys. Discuss., https://doi.org/10.5194/acp-2018-1366
Manuscript under review for journal Atmos. Chem. Phys.
Discussion started: 15 February 2019

Atmospheric Chemistry and Physics Discussions

are responsible for ROS generation on particle surface (McWhinney et al., 2013b;Li et al., 2003), more work is still required to deeply understand the toxicity of soot and the reason why the toxicity varies greatly among different soot samples. On the other hand, soot particles are prone to undergo oxidation by O_3, OH and NO_3 etc. during transport in the atmosphere. Subsequently, functionalization including formation of OH, C=O, epoxide (C-O-C) and COOH occurs (Mawhinney et al., 2000;Liu et al., 2015;Holder et al., 2012). This make it more complicate to understand the toxicity of soot particles. For example, several studies have found that atmospheric relevant oxidation of CB or BC by O_3 leads to enhancement of their oxidative potential (Li et al., 2009;Li et al., 2013;Li et al., 2015;Antinolo et al., 2015;Holder et al., 2012). In particular, the DTT decay rate of soot particles has been found increasing as a function of the content of quinone formed via ozone oxidation of organic carbons in soot (Antinolo et al., 2015). However, some other studies have found that oxidation of CB or soot by O_3 or OH under atmospheric related conditions has little influence on their oxidative potential or cytotoxicity although surface functionalization is observable (Liu et al., 2015;Peebles et al., 2011). Therefore, it is necessary to understand the role of functional groups in the toxicity of soot particles.

During combustion process, however, multiple functional groups including OH, C=O, COOH, esters and so on are usually formed at the same time and present in both OC and EC (Han et al., 2012a). Thus, it is difficult to differentiate the role of one kind of functional group from others in the toxicity of soot particles. Carbon black (CB), which is produced from incomplete combustion of heavy petroleum materials under

controlled conditions (Apicella et al., 2003), and engineered carbon nanomaterials are a quasi-graphitic form of nearly pure element carbon (EC, consist of graphene layers) and are distinguished by its very low quantities of extractable organic compounds and total inorganics (Long et al., 2013) compared with soot. Therefore, it is possible to investigate the role of functional groups in the toxicity of soot when using CB or engineered carbon particles with different functional groups as model sample of soot particles. Actually, it has been recognized that the surface properties of carbon nanomaterials will influence their biological effects or toxicity (Lara-Martinez et al., 2017;Liu et al., 2014b;Koromilas et al., 2014). For example, a recent study has found that hydrated graphene oxide exhibited a higher cytotoxicity to THP-1 and BEAS-2B cells as a consequence of lipid peroxidation of the surface membrane and membrane lysis compared to pristine and reduced graphene oxide (Li et al., 2018). Functionalized multiwalled carbon nanotubes (fMWCNTs) is highly cardioembryotoxic in comparison with Functionalized oxygen-doped multiwalled carbon nanotubes (fCOxs) (Lara-Martinez et al., 2017). As pointed out by Lara-Martinez et al. (2017), however, cytotoxic effects of carbon nanomaterials at the cellular level generate considerable controversy and more research is clearly needed to gain insight into the mechanism of these adverse effects. In addition, passive diffusion and energy-dependent endocytosis are the two methods suggested for particles entry into living cells. They can also be distributed to various parts of the body, from where they can either remain, translocate, or be excreted. Therefore, it is meaningful to investigate the influence of functionalization on other endpoints alone even for these carbon nanomaterials.

Atmos. Chem. Phys. Discuss., https://doi.org/10.5194/acp-2018-1366
Manuscript under review for journal Atmos. Chem. Phys.
Discussion started: 15 February 2019

In the current study, both the cell-free toxicity and the cell cytotoxicity of carbon nanomaterials with different functionalities were evaluated to focus on the role of functionalization in their toxicities to understand the possible influence of different source or oxidation processes on the toxicity evolution of soot particles during transport in the atmosphere. DTT decay rate representing the oxidative potential and the cytotoxicity of murine macrophage cell were investigated. The carbon nanomaterials were characterized with inductively coupled plasma-mass spectrometry (ICP-MS), thermal gravity analysis (TGA), X-ray photoelectron spectroscopy (XPS), transmission electron microscopy (TEM) and zeta potential analyzer. The role of oxygen containing species in the toxicity of carbon nanomaterials was discussed. This work will be helpful for understanding the toxicity evolution of soot during oxidation in the atmosphere and evaluation the toxicity of engineered nano-particles.

Experimental Section

Chemicals and characterization of particle samples. Commercial carbon nanomaterials including Special Black 4A (SB4A), graphene, graphene oxide, SWCNT, SWCNT-OH and SWCNT-COOH were used in this study. All these functional groups have been identified in soot particles and chemical aged soot or CB particles. SB4A was supplied by Degussa. The other carbon nanomaterials with purity >98% were supplied by Timesnano. To obtain graphene oxide with low epoxide content, graphene oxide were thermally treated at 200 °C for 30 min in high purity (99.999%) nitrogen flow. Dithiothreitol (DTT) was supplied by Sigma-Aldrich. 5,5′-dithiobis-(2-nitrobenzoic acid) (DTNB) was obtained from Alfa Aesar. Standard solutions of metal

ions including Cr, Mn, Fe, Co, Ni, Cu, Zn, Cd, As, Sn and Pb were supplied by National Institute of Metrology, China. 30 % H_2O_2 solution was supplied by Sinopharm Chemical Reagent Co., Ltd.

A transmission electron microscope (H-7500, Hitachi) was used to investigate the morphologies of carbon nanomaterials. Particles were ultrasonically dispersed in ultrapure water (18 MΩ) and a droplet of suspending liquid was deposited onto a Cu microgrid. An acceleration voltage of 80 kV was used for measurements. The morphologies were shown in Fig. S1. The diameter of primary particles were analyzed by ImageJ 1.41 software (Liu et al., 2010). The diameter of the primary carbon sphere for SB4A was 66±17 nm SB4A. The out diameter (OD) of SWCNT, SWCNT-OH and SWCNT-COOH was <2 nm with fiber length of 1-3 μm according to the product report and also confirmed by TEM (Fig. S1). Graphene and graphene oxide were 2-dimensional materials with monolayer and the diameter of 0.5-3 μm.

XPS were measured using an AXIS Supra/Ultra (Kratos, Kratos Analytical Ltd.) to identify the oxygen containing species on the surface of carbon nanomaterials. The samples were excited by Al Kα X-ray ($h\nu$=1486.7 eV) with 15 kV of working voltage and 40 mA of emission current. The spectra were analyzed with XPS Peak software. The content of organic carbon (OC) in carbon nanomaterials was measured by thermal desorption using a commercial TG instrument (TGA/DSC1/HT1600, Mettler-Toledo Co., Ltd.). The amount of OC lost from the particles was recorded when the temperature was ramped from 30 to 300 °C at 10 °C min^{-1} in nitrogen flow according to the protocol reported in previous work (Han et al., 2012a). Metals in the particles were measured

Atmos. Chem. Phys. Discuss., https://doi.org/10.5194/acp-2018-1366
Manuscript under review for journal Atmos. Chem. Phys.
Discussion started: 15 February 2019

147 with an inductively coupled plasma mass spectrometer (ICP-MS 7500a, Agilent
148 Technologies) after digested with concentrated 1:3 HNO_3/HCl. Transition metals were
149 quantified with the standard solution. Zeta potentials of the carbon nanomaterials were
150 measured after sonicating 30 min in ultrapure water (18.2 MΩ) by using a Nanoparticle
151 Size & Zeta Potential Analyzer (Zetasizer Nano, ZS90).
152 **DTT assay test.** The DTT assay is an indirect chemical assay used for measuring the
153 redox cycling capacity of PM. The added DTT is oxidized to its disulfide form by the
154 ROS in particulate matter (Kumagai et al., 2002). Thus, the rate of DTT consumption
155 is proportional to the concentration of the ROS in the sample (Cho et al., 2005). In this
156 study, ~150 μg carbon nanomaterials were suspended in 10.0 ml phosphate buffer (0.1
157 M, pH 7.4) and sonicated for 15 min. 2.0 ml of 0.5 mM DTT solution was added to 3.0
158 ml aliquots of the sonicated suspensions. A redox reaction took place in a thermostat
159 shaking chamber at 37 ºC. The remained DTT concentration was measured every 15
160 minutes by adding 0.25 ml of the reaction mixture filtration to 1.0 ml of 0.25 mM
161 DTNB solution. DTNB reacted with the thiol groups in DTT to form a yellow
162 compound (2-nitro-5-thiobenzoate, NTB), which could be detected by UV-vis
163 absorption spectrometer (723N, Shanghai Ruiting Technology Co., Ltd) at 412 nm.
164 Then, the amount of DTT consumed by PM was calculated according to the standard
165 curves of DTT. The loss rate of DTT via a redox reaction in the presence of PM was
166 monitored as the concentration decrease of DTT and normalized to the particle mass.
167 Blank experiments were carried out without carbon nanomaterial particles in the buffer
168 solution. For some samples, the response to the DTT assay was also measured for the

water soluble components of SWCNT by filtering aliquots of the samples with a 0.22 μm syringe PTFE filter, and measuring the activity of the solution without particles.

In vitro assays. Carbon nanomaterial particles were dispersed with 0.025% Tween-80 in 0.19% NaCl solution using a Dounce glass homogenizer, followed by sonication. A homogeneous and stable suspension of SWCNTs was obtained after the sonication process. Cytotoxicity assessment of carbon nanomaterials was carried out using the murine J774 cells. Three different assays targeting distinct mechanisms of cellular metabolic perturbations were assessed simultaneously, including ATP (energy metabolism), LDH (membrane integrity) and BrdU (incorporation into DNA) assays. The experiments were carried out according to the corresponding protocol. Briefly, 4×10^5 J774 cells ml^{-1} were exposed to carbon particles in 96-well plates for 24 hours for ATP and LDH assays, while the initial J774 cell concentration was 2×10^5 cells ml^{-1} for BrdU assay. Carbon nanomaterials were dosed at 0, 10, 30 and 100 μg cm^{-2} in a final volume of 200 μl $well^{-1}$ as similar to that reported in literatures (Kumarathasan et al., 2014;Kumarathasan et al., 2012). The luminescence spectroscopy of the supernatant after centrifugal separation at 1000 rpm for 5 min was measured after 24 h of cell exposure using a Multimode Microplate Reader (Varioskan®Flash, Thermo Fisher Scientific). The zero dose of carbon nanomaterials referred to the blank experiment and also means the toxicity of 0.025% Tween-80 alone in 0.19% NaCl solution. Similar to the literature results (Hadrup et al., 2017), they did not incur any obvious deleterious effect on cells growth. In addition, it has been well recognized that carbon nano-particles tended to aggregate in water even after ultrasonic dispersion. Tween-80 has

Atmos. Chem. Phys. Discuss., https://doi.org/10.5194/acp-2018-1366
Manuscript under review for journal Atmos. Chem. Phys.
Discussion started: 15 February 2019

been verified to be a biocompatible dispersant for carbon black (Kim et al., 2012). Negative control experiments were performed in wells containing medium without cells to obtain a value for background luminescence. Positive control experiments were carried out with H_2O_2 solution for LDH assays (Fig. S2).

Results and discussion

Oxidative potential of carbon nanomaterials. Figure 1 shows the DTT decay rates of SB4A, graphene, graphene oxide, SWCNT, SWCNT-OH and SWCNT-COOH. They were 45.9±3.0, 58.5±6.6, 160.7.0±21.7, 38.9±8.9, 57.0±7.2 and 36.7±0.2 pmol $min^{-1}\mu g^{-1}$, respectively. Except for graphene oxide, the measured DTT decay rates for these carbon nanomaterials (with mean value of 47.4±10.1 pmol $min^{-1}\mu g^{-1}$) were comparable with the DTT loss rates of BC reported in the literatures. For example, it was 36.2±4.9 pmol min^{-1} μg^{-1} for Printex U (Li et al., 2015) and 59.3±7.4 pmol min^{-1} μg^{-1} for SWCNT (Liu et al., 2015). These values were also comparable with that of the typical soot particles (BC), such as 33.6 pmol min^{-1} μg^{-1} for methane flame soot (Holder et al., 2012), 49±7 pmol min^{-1} μg^{-1} for propane flame soot (Antinolo et al., 2015), 27.0 pmol min^{-1} μg^{-1} for hexane flame soot (Li et al., 2013), as well as the typical ambient $PM_{2.5}$ particles (34.7±19.1 pmol min^{-1} μg^{-1}) (Charrier and Anastasio, 2012;Liu et al., 2014a). However, the measured DTT decay rates for these carbon nanomaterials were significantly higher than that of diesel soot (6.1 pmol min^{-1} μg^{-1}) and graphite (0.9 pmol min^{-1} μg^{-1}) (Li et al., 2013) reported in previous work. It should be noted that the DTT decay rate of graphene oxide measured in this study was 160.7±21.7 pmol min^{-1} μg^{-1}. Based on T-test, the DTT decay rate of graphene oxide was significantly higher than that of other

Atmos. Chem. Phys. Discuss., https://doi.org/10.5194/acp-2018-1366
Manuscript under review for journal Atmos. Chem. Phys.
Discussion started: 15 February 2019

tested carbon nanomaterials at the 0.05 level (t=8.498, which is greater than the critical value of 2.447). This means that graphene oxide definitely has a stronger oxidative potential than other CB or carbon nanomaterials in this work.

Cytotoxicity of carbon nanomaterials to murine J774 cell line.

At the present time, the A549 (a human adenocarcinomia alveolar epithelial cell) and THP-1 (a human leukemia monocytic cell line) cell lines were usually chosen as target cell lines (Kumarathasan et al., 2012;Kumarathasan et al., 2014;Liu et al., 2015) to evaluate the alveolar and pulmonary toxicity of CB particles. As the first barrier of the immune system, macrophage cell lines will fight against the invaded particles in the lungs. Macrophage cell lines like J774 cells are ideal model systems for establishing the biophysical foundations of autonomous deformation and motility of immune cells (Lam et al., 2009). It has been found that CB nanoparticles are able to stimulate the release of macrophage chemo-attractants when exposed to type II epithelial cell lines (L-2 cells) at sub-toxic doses (Barlow et al., 2005). CNTs exposure can also lead to biological changes in J774 cells (Kumarathasan et al., 2012). Therefore, it is meaningful to investigate the cytotoxicity of different carbon nanomaterials as well as the influence of surface functional group on the macrophage cell lines.

Figure 2 shows the in vitro toxicities of SB4A, graphene, graphene oxide, SWCNT, SWCNT-COOH and SWCNT-OH. The stars mean the indicator of the toxicity at a certain dose of carbon nanomaterials is significantly different from the corresponding blank experiments at 0.05 level. As shown in Fig. 2, the metabolic activity of J774 cell line decreased monotonously as a function of the dose of all these carbon nanomaterials.

This means the carbon nanomaterials investigated in this work are toxic to murine J774 cell line. This is consistent with the previous results that CNT and Printex U are toxic to J774 cells (Kumarathasan et al., 2012) and graphene oxide can induce dose-dependent cell death in normal lung fibroblasts (HLF), macrophages (THP-1 and J744A), epithelial (BEAS-2B) cells, lung cancer cells A549 etc. (Zhang et al., 2016;Li et al., 2018).

In Fig. 2A, the relative ATP level (1.01±0.02) at the SB4A dose of 10 μg cm^{-2} was almost the same as that of the blank sample, while it significantly decreased to 0.89±0.05 and 0.61±0.07 when the dose of SB4A increased to 30 μg cm^{-2} and 100 μg cm^{-2}, respectively. Similarly, the relative ratio of BrdU incorporation decreased from 0.74±0.03 to 0.60±0.04 when the dose of SB4A increased from 30 to 100 μg cm^{-2}. This means SB4A is also an inhibitor for cell proliferation of murine J744. However, the released LDH levels were constant within experiment uncertainty at different SB4A doses. This means the cell membrane might be intact when exposed to SB4A.

As shown in Fig. 2B-F, the metabolic activity of murine J774 cell decreased more significantly when exposed to engineered carbon nanomaterials than SB4A. For example, the relative ratio of ATP level was 0.67±0.06, 0.84±0.03, 0.59±0.10, 0.93±0.01 and 0.88±0.02 even when the J774 cells were exposed to 10 μg cm^{-2} graphene, graphene oxide, SWCNT, SWCNT-OH and SWCNT-COOH, respectively. When exposed to high doses of engineered carbon nanomaterials, the reduction of relative ATP level became more significant. These results mean the cytotoxicity of the engineered carbon nanomaterials studied in this work are stronger than that of SB4A

Atmos. Chem. Phys. Discuss., https://doi.org/10.5194/acp-2018-1366
Manuscript under review for journal Atmos. Chem. Phys.
Discussion started: 15 February 2019

257 regarding to metabolic activity. Graphene, graphene oxide and SWCNT-COOH
258 significantly enhanced release of LDH at different exposure levels, while SWCNT and
259 SWCNT-OH only led to significant increases of released LDH at high exposure level
260 (100 μg cm^{-2}). This implies the integrity of cell membrane decreased when J774 cells
261 were exposed to these engineered carbon nanomaterials. This might be related to lipid
262 peroxidation induced by these particles (Li et al., 2018).

263 It should be noted that the reduction of ATP ratio of J774 cells exposed to graphene
264 oxide was weaker than that of graphene. The reduction of ATP ratio of J774 cells
265 exposed to SWCNT-OH or SWCNT-COOH was also weaker than that of SWCNT.
266 However, compared with graphene, graphene oxide showed much stronger toxicity to
267 J774 cell as far as the membrane integrity was considered. The released LDH at
268 exposure level of 30 μg cm^{-2} graphene oxide was comparable with that when exposed
269 to 150 ppm H_2O_2 (Fig. S2). In addition, graphene oxide, SWCNT-OH and SWCNT-
270 COOH significantly inhibited DNA synthesis of J774 cells when the carbon
271 nanomaterials doses were above 10 μg cm^{-2}, while graphene and SWCNT did not show
272 significant inhibition of DNA synthesis for J774 cells. For instance, the relative ratio of
273 BrdU when J774 cells exposed to 100 μg cm^{-2} of graphene oxide was 0.61±0.10, while
274 it was 0.77±0.10 for graphene exposed cells at the same exposure level. They were
275 0.62±0.10 for SWCNT-OH and 0.56±0.09 for SWCNT-COOH treated cell at a dose of
276 10 μg cm^{-2} compared with 0.83±0.09 for 10 μg cm^{-2} of SWCNT treated J774 cell. These
277 results suggested that functionalized carbon nanomaterials caused a low cytotoxicity of
278 murine J774 cell line regarding to the cell apoptosis, while a stronger toxicity was

demonstrated for cell proliferation and the membrane integrity. This finding was true, in particular, for graphene oxide.

Influence of physiochemical properties on the toxicity of different samples. It should be pointed out that the morphologies of these carbon nanomaterials varied greatly. SB4A was a zero dimensional material. SWCNT, SWCNT-OH and SWCNT-COOH were one dimensional materials. Graphene and graphene oxide were two dimensional materials (Fig. S1). The DTT decay rate (Fig. 1) did not show obvious dependence on their morphologies in this work. For example, except for graphene oxide, the DTT decay rates were comparable among all the other materials regardless of the morphology. Graphene and graphene oxide showed similar particle size, graphene layer and morphologies (Fig. S1), while they showed totally different toxicity as shown in Fig. 1. In Fig. 2, the cytotoxicity of SB4A, graphene and SWCNT showed an increase trend regarding the metabolic activity of J774 cell. This can be explained by the different mode of action (MOA) when the cells were exposed to different types of nanomaterials. For example, adhesions and/or covering on cells could be the main MOA for graphene/graphene oxide (2-D structure), while for carbon nanotubes (1-D structure), piercing and/or internalization by cells could be the main MOA. This means morphology should plays a role in determining the cytotoxicity of the carbon nanomaterials studied in this work. Therefore, in the following section we mainly discuss the cytotoxicity among these materials having same dimension, such as SWCNT-OH and SWCNT-COOH verse SWCNT and graphene oxide verse graphene. In addition, as shown in Fig. S3, all these carbon nanomaterials revealed negative zeta

potential from -42 mV to -20 mV. SB4A, graphene oxide and SWCNT-COOH almost borne the same zeta potential (-42 mV), while SWCNT, SWCNT-OH and graphene showed comparable zeta potential. This observation suggested the stability of dispersed SB4A, graphene oxide and SWCNT-COOH in water and the interaction between these particles with cells was comparable.

Transition metals in the particles have been identified to be the important contributor to ROS generation (McWhinney et al., 2013b;Li et al., 2003). The content of transition metals including Cr, Fe, Mn, Co, Ni, Cu, Zn, As, Cd, Sn and Pb were measured by using an ICP-MS after the carbon nanomaterials were digested with 1:3 HNO_3/HCl. As shown in Fig. S4A, Fe was the most abundant transition metal in these carbon nanomaterials. Its concentration varied from 122 μg g^{-1} to 6596 μg g^{-1} among different carbon nanomaterials. The concentration of other metals varied from zero to several hundred μg g^{-1} depending on both carbon nanomaterials and the type of metals. Compared with SB4A, these engineered carbon nanomaterials showed higher metal content. For example, the total metal content in graphene was 6 times as high as that in SB4A, while it was 33 times in SWCNT as high as that in SB4A. This can be explained by the fact that graphene and SWCNT materials were catalytically synthetized using metal catalysts containing Fe, Co or Ni. It should be noted that although the metal content of SB4A was very low compared with other materials, the DTT decay rate of SB4A was still comparable with these engineered carbon nanomaterials except for graphene oxide as shown in Fig. 1. On the other hand, SWCNT had the highest metal content, while graphene oxide rather than SWCNT showed the strongest DTT decay

rate. In addition, the soluble metal contents were in the following order: SWCNT-COOH > SWCNT > SB4A > graphene oxide > graphene > SWCNT-OH (Fig. S4B), after being sonicated for 30 min in water. Graphene oxide (103.7 μg g^{-1}) did not show a significant difference compared with SB4A (106.3 μg g^{-1}) and graphene (93.7μg g^{-1}). These results indicated that the high oxidative potential of graphene oxide relative to other materials cannot be attributed to their difference in bounded or soluble transition metals. This can be explained by the following reasons. First, metal content were measured after digested with 1:3 HNO_3/HCl. The speciation of metals should be quite different from that presenting in the pristine carbon nanomaterials. For example, the contents of soluble metal ions after sonicated for 30 min (Fig. S4B) varied from zero to 356 μg g^{-1}. These values were much lower than the corresponding metal contents of digested samples as shown in Fig. S4A. Second, metal might be in the inner pores of carbon nanomaterials. This will decrease the efficiency of metals to generate ROS. Finally, the concentration of carbon nanomaterials was 10-40 μg ml^{-1} in DTT assay tests. This meant the concentration of transition metals was at ng ml^{-1} level even if all of the transition metals were available. The low concentration of metals released might lead to negligible contribution to ROS formation. This was further confirmed by the very small DTT decay rate of the SWCNT filtered solution (1.66±0.15 pmol min^{-1} μg^{-1}) compared with that of SWCNT suspension (38.9±8.9 pmol min^{-1} μg^{-1}) even though SWCNT had the highest metal concentration (Fig. S4A). This was consistent with the previous conclusions that redox activity originates from the particle surface of CB or BC materials but not from water-soluble substances (Liu et al., 2015;McWhinney et al.,

345 2013a).

346 Figure 3 shows the thermo gravity and differential thermal analysis curves for these
347 CB materials when the temperature was ramped from 30 to 300 °C at 10 °C min^{-1} in
348 nitrogen flow. Weight loss (Fig.3A) accompanied with an endothermic process (Fig. 3B)
349 were observed below 60°C for all of these samples. This can be ascribed to desorption
350 of surface adsorbents including organics and trace water. As shown in Fig. 3B, the
351 saddle points of these differential thermal analysis curves were observed at 35, 35, 41,
352 42, 56 and 58 °C for graphene, SWCNT, SB4A, SWCNT-OH, SWCNT-COOH and
353 graphene oxide, respectively. It should be noted that the oxidized carbon nanomaterials
354 such as SWCNT-OH, SWCNT-COOH and graphene oxide showed higher saddle points
355 of the heat curves than graphene, SWCNT and SB4A. This implies stronger interaction
356 between the adsorbents and these three oxidized carbon nanomaterials compared with
357 the counterpart. Therefore, it is reasonable to deduce that the adsorbed water mainly
358 contribute to the weight loss in this stage. The sample weight slightly decreased as the
359 temperature further increased for all of these carbon nanomaterials except for graphene
360 oxide and accompanied with a gradual increase of the heat flow. This can be ascribed
361 to desorption of adsorbed organics from the surface of the carbon nanomaterials. The
362 relative small increase rate of the heat in this stage was consistent with the small heat
363 capacity of organics when compared with the first one which was ascribed to desorption
364 of water. For graphene oxide, however, weight loss (from 32% to 60%) was
365 significantly observed accompanied with an acute exdothermic process when the
366 temperature increased from 150 to 200 °C as shown in Fig. 3B. This implies that release

Atmos. Chem. Phys. Discuss., https://doi.org/10.5194/acp-2018-1366
Manuscript under review for journal Atmos. Chem. Phys.
Discussion started: 15 February 2019

of pyrolysis products and structure collapse of graphene oxide occur. It also means a high reactivity of graphene oxide and highlights the distinctive property of graphene oxide among these investigated carbon nanomaterials.

The adsorbed organics were estimated based on the thermogravimetric curves when the possible contribution of water was ruled out. For graphene oxide, 150 °C was taken as the endpoint, while 300 °C was chosen for other samples. The content of adsorbed organics on SB4A, graphene, graphene oxide, SWCNT, SWCNT-OH and SWCNT-COOH was 6 %, 13 %, 15 %, 9 %, 5 % and 9 %, respectively, as shown in the insert graph of Fig. 3A. The content of organics cannot explain the sequence of the DTT loss rate (Fig. 1) and the cytotoxicity (Fig. 2) of these carbon nanomaterials. For example, the content of organics on graphene and graphene oxide were almost the same, while the DTT decay rate of graphene oxide was as about 2.5 times as that of graphene (Fig. 1) and the cytotoxicity of graphene oxide as for metabolic activity to murine J774 was weaker than that of graphene. In addition, the organic content of SWCNT was the same as that of SWCNT-COOH, while SWCNT-COOH showed weaker toxicity to murine J774 cell line than SWCNT as far as the metabolic activity was considered (Fig. 2). This means the different toxicities observed in this study cannot be explained by the adsorbed organics among these materials.

To further investigate the role of surface oxygen in the toxicity of carbon nanomaterials, the oxygen-containing species of these carbon nanomaterials were identified with X-ray photoelectron spectroscopy. Fig. 4 shows the typical O1s and C1s spectra of these carbon nanomaterials. Adsorbed oxygen at 535.2 eV, carbon-oxygen

single bond in hydroxyl group (C-OH) at 533.5 eV, carbon-oxygen single bond in epoxide (C-O-C) at 532.6 eV, carbon-oxygen double bound (C=O) at 531.8 eV and highly conjugated form of carbonyl oxygen such as quinone groups at 530.5 eV (Schuster et al., 2011) presenting in these CB samples as shown in Fig. 4A-F. In the C1s spectra (Fig. 4G-L), the band at 291 eV was attributed to the shakeup peak associated with π-π* transition (Simmons et al., 2006). The band at 289 eV corresponded to carbonyls and epoxides was observed at 287 eV (Kuznetsova et al., 2001). The band at 285 eV and 284.6 eV was assigned to graphite and sp^3 carbon, respectively. In particular, the intensity of C-O-C at 532.6 eV in graphene oxide was very strong compared with other carbon nanomaterials. At the same time, the band of C-O-C at 287 eV was also much stronger than that of other carbon nanomaterials in the C1s spectrum. These results mean that epoxides (C-O-C) is the predominate species (Fig. 5C and I) in graphene oxide.

Fig. 5A summarizes the distribution of the oxygen species mentioned above normalized to O atoms in these carbon nanomaterials. Highly conjugated form of carbonyl oxygen (quinone) and adsorbed oxygen contributed little to the total oxygen on the surface (<1 %), while C=O, C-O-C and C-OH were predominate oxygen-containing species. Our results agree well with the previous work that C=O, C-O-C and C-OH dominated oxygen-containing species on natural chars, diesel soot, hexane soot and activated charcoal (Langley et al., 2006). Although quinone has been well recognized to contribute to ROS generation on the surface of fine particles (Kumagai et al., 2002;Li et al., 2002b), the content of quinone was lower than 0.35% and showed

411 little difference among all of these tested carbon nanomaterials (Fig. 5A and B). It did
412 so for adsorbed oxygen content. Therefore, we can conclude that the very large DTT
413 decay rates of graphene oxide compared with other carbon nanomaterials as shown in
414 Fig. 5C cannot be explained by the content of quinone or adsorbed oxygen.

415 As shown in Fig. 5A, the total oxygen content of SB4A, graphene, SWCNT,
416 SWCNT-OH and SWCNT-COOH was 6.68%, 2.41 %, 2.88%, 3.60% and 9.21%,
417 respectively. They were comparable with that of diesel soot (2.1%-12.2%) (Schuster et
418 al., 2011). However, the oxygen content of graphene oxide (29.0%) was significantly
419 higher than the other carbon nanomaterials (Fig. 5A). At the same time, the distribution
420 pattern of the surface species on graphene oxide was quite different from the other
421 carbon nanomaterials. Fig. 5B compared the content of the oxygen-containing species
422 of graphene oxide with other carbon nanomaterials. The red stars indicate the content
423 of oxygen-containing species in graphene oxide, while the blue boxes show that of other
424 carbon nanomaterials. It can be seen that the content of quinone and adsorbed oxygen
425 showed no difference between graphene oxide and other carbon nanomaterials. The
426 concentration of C=O and C-OH in graphene oxide was slightly higher than that in the
427 other carbon nanomaterials. However, the content of epoxide in graphene oxide was
428 significantly higher than the other carbon nanomaterials. The content of epoxide in
429 graphene oxide normalized to O atoms was 20.8 %, which was 71.7 % of its total
430 oxygen content (Fig. 5B), while it was less than 2.7 % in other carbon nanomaterials.
431 This well corresponded to the large DTT decay rates of graphene oxide (160.7 pmol
432 min^{-1} μg^{-1}) compared to other carbon nanomaterials (less than 60 pmol min^{-1} μg^{-1}) as

Atmos. Chem. Phys. Discuss., https://doi.org/10.5194/acp-2018-1366
Manuscript under review for journal Atmos. Chem. Phys.
Discussion started: 15 February 2019

433 shown in Fig. 5C. It should be noted that the content of epoxide was not linearly
434 correlated to the DTT activity. This can be explained by the typical nonlinear
435 relationship between the dose of toxicant and toxicity (Antinolo et al., 2015). It should
436 be pointed out that multiple parameters of particle may have influence on its toxicity,
437 in particular, on the cytotoxicity. For example, particle size and morphology may have
438 influence on the material mobility and uptake by cells. However, the above results at
439 least imply that these physiochemical properties such as morphology, metal and OC
440 content should not be crucial factors as for the toxicity of these carbon nanomaterials
441 because it is difficult to observe an obvious dependence of the toxicity on these factors.
442 In the meantime, we can propose that epoxides in graphene oxide are mainly
443 responsible for the high ROS activity of graphene oxide. The high ROS formation
444 potential of graphene oxide might also explain its strong cytotoxicity to J774 cell line
445 regarding to the cell membrane.

446 To further confirm this assumption, we measured the ROS activity of the thermally
447 treated graphene oxide at 200 °C in nitrogen flow because C-O-C (epoxide) structure
448 can be broken under this condition as shown in Fig. 3 and discussed above. XPS spectra
449 confirmed the broken of epoxide by the fact that the content of epoxide in thermally
450 treated graphene oxide decreased to 4.3% from 20.9% in graphene oxide as shown in
451 Figs. S5 and S6. In addition, TEM results also showed that graphene oxide broke into
452 small sheets, whose morphology and particle size were close to that of SB4A and
453 graphene oxide or graphene (Fig. S1). At the same time, the DTT decay rate of the
454 thermally treated graphene oxide decreased to 54.9±9.8 pmol min^{-1} μg^{-1} (Fig. 6). This

455 value was comparable to the DTT decay rates of other carbon nanomaterials, in
456 particular, graphene (58.5±6.6 pmol min^{-1} μg^{-1}) (Fig. 1), while it was significantly lower
457 than the graphene oxide (160.7.0±21.7 pmol min^{-1} μg^{-1}) as shown in Fig. 6. It should
458 be noted the total oxygen contents of thermally treated graphene oxide was 19.3 %,
459 which was lower than that of graphene oxide (29.0 %) but significantly higher than that
460 of other carbon nanomaterials. However, the DTT decay rate of thermally treated
461 graphene oxide was still comparable with other carbon nanomaterials. This further
462 highlights the importance of functional group in the toxicity. Therefore, it means that
463 epoxides in graphene oxide are the highly reactive site for ROS formation on the surface
464 of graphene oxide. This is for the first time to observe that epoxide is a highly reactive
465 site for ROS formation besides quinone on carbon nanomaterials. This result is also
466 well consistent with the previous founding that epoxides in graphene oxide can oxidize
467 SO_2 to sulfate (He and He, 2016).

468 However, we did not observed significant dependence of cytotoxicity to murine
469 J774 cell line and the content of oxygen-containing species on the surface of carbon
470 nanomaterials although oxidized CB materials showed reduced toxicity to J774 cell
471 lines as far as metabolic activity was considered. In particular, the difference in surface
472 oxygen content between graphene oxide and graphene was much higher than that
473 between SWCNT-OH/SWCNT-COOH and SWCNT (Fig. 5A), while the differences in
474 metabolic activity to J774 cell line between graphene oxide and graphene was similar
475 to that between SWCNT-OH/SWCNT-COOH and SWCNT. The pathways of cellular
476 toxicity induced by particles reside in both oxidative stress (ROS) and non-oxidative

477 stress dependent (Shvedova et al., 2012). Oxidative stress leads to selective oxidation
478 of mitochondrial CL, NADPH oxidase activation and MPO activation in neutrophils,
479 while non-oxidative stress results from interference with mitotic spindle and actin
480 cytoskeleton, and steric hindrance of ion channels. The interaction between target cells
481 and particles should be much complicated than that between DTT and particles. As
482 discussed above, the cytotoxicity of nano-particles relied on not only the mode of action
483 but also the chemical nature of particles. Therefore, the different responses of the
484 oxidation potential and the cytotoxicity to the epoxide content in these carbon materials
485 might be accounted for by different mechanisms of toxicity among these assays.

486 **Conclusion ad atmospheric implications**

487 The DTT decay rates of special black 4A (SB4A), graphene, graphene oxide, single
488 wall carbon nanotubes (SWCNT), SWCNT-OH and SWCNT-COOH were 45.9±3.0,
489 58.5±6.6, 160.7±21.7, 38.9±8.9, 57.0±7.2 and 36.7±0.2 pmol $min^{-1}\mu g^{-1}$, respectively.
490 Epoxide has been for the first time identified as a highly active functional group in the
491 carbon nanomaterials as far as the oxidation potential is considered.

492 Oxidation is a useful method to obtain functionalized CB materials with distinctive
493 performance in industry. It is also a primary process in the atmosphere relating to
494 chemical aging of particles including soot and CB particles. This process unusually
495 leads to formation of carbonyls, hydroxyls, carboxylic acids, esters, ethers and epoxides
496 on the surface of CB or BC particles. Previous work have found that oxidation of carbon
497 nanomaterials (SWCNT) by O_3 or OH under atmospheric related conditions has little
498 influence on their oxidative potential or cytotoxicity although carbonyls, carboxylic

499 acids and esters were formed (Liu et al., 2015). Similarly, surface functionalization was
500 observed for commercial CB materials by ozone oxidation, while increase in the
501 cytotoxicity of murine macrophages and release of inflammation markers upon
502 exposure to the oxidized CB were not observed (Peebles et al., 2011). However, some
503 other studies observed that oxidation process enhanced the oxidation potential (Li et al.,
504 2015;Li et al., 2013;Antinolo et al., 2015) as well as the cytotoxicity (Holder et al.,
505 2012) of CB and BC particles. Using the model carbon nanomaterials with different
506 dominate surface functionalities in this work, we have found that hydroxyl and carboxyl
507 functionalized CB particles had little influence on their oxidation potential, while
508 epoxide functionalized CB (graphene oxide) led to a very strong oxidation potential.
509 Epoxide has been identified as a surface product on SWCNT when treated with high
510 concentration of ozone (Mawhinney et al., 2000;Yim and Johnson, 2009). Besides
511 carboxylic acids, esters (Liu et al., 2015), ketone, lactone and anhydride species (Liu et
512 al., 2010;Han et al., 2012b), epoxides has also been identified as the surface product
513 during oxidation of SWCNT in atmosphere relevant conditions (Liu et al., 2015). This
514 means that oxidation potential enhancement of CB particles is also possibly resulted
515 from the formation of epoxide during chemical aging in the atmosphere. On the other
516 hand, graphene oxide was an important commercial product, while showed strong
517 oxidation potential as observed in this work. Therefore, Mussel-inspired chemistry is
518 necessary for fabrication of functional materials and decreasing their toxicity and for
519 biomedical applications (Liu et al., 2014b;Zhang et al., 2012).

520 It has been found that CB particles (Printex 90) can induce opening of plasma

membrane calcium channels leading to a calcium influx and cause significant release of proinflammatory cytokine TNF-α by the murine J774 cells (M. et al., 2004), subsequently potentially induce migration of macrophages (Barlow et al., 2005). This could initiate the recruitment of inflammatory cells to sites of particle deposition and the subsequent removal of the particles by macrophages. The metabolic activity of these hydroxyl, carboxylic acid and epoxide functionalized carbon nanomaterials increased when compared with the corresponding sample as observed in this work. This implies chemical aging of these carbon nanomaterials might not pose an enhanced cytotoxicity risk to macrophages although the oxidized carbon nanomaterials were still toxic as far as metabolic activity was considered. However, the oxidized carbon nanomaterials might pose enhanced cytotoxicity to macrophages regarding to membrane integrity and DNA synthesis. It should be pointed out that exposure experiments were performed under high particle concentration with short exposure time in this work. More work needs to be done at low particle concentration with long exposure time in the future. On the other hand, it has been found that aging rate of BC particles under highly polluted urban environment is faster than that under clean conditions (Peng et al., 2016). In the future, much work should be performed on the toxicity evolution of CB or BC particles under real atmospheric conditions. Finally, it should be noted that the interaction between particles and biological entities such as proteins or cells has not been considered in this work. Therefore, the in vivo toxicological effect of these functionalized particles needs to be further evaluated in the future.

AUTHOR INFORMATION

543 Corresponding Author

544 *E-mail: liuyc@buct.edu.cn, phone: +86-10-68471480, fax: +86-10-68471480 or

545 sjliu@rcees.ac.cn,

546

547 **AUTHOR CONTRIBUTION**

548 Y. L., H. H. and S. L. designed the experiments. Y. L. wrote the paper. Y. L., H. J. and

549 Y. G. did the DTT assay tests. C. L. and L. W. did the cytotoxicity assessments. H. J.

550 and B. Z. performed the characterization of samples.

551

552 **ACKNOWLEDGMENTS**

553 This research was financially supported by the National Natural Science Foundation of

554 China (91543109). YCL should thank Beijing University of Chemical Technology for

555 financial supporting.

556 **References:**

557 Antinolo, M., Willis, M. D., Zhou, S., and Abbatt, J. P. D.: Connecting the oxidation of soot to its redox
558 cycling abilities, Nat Commun, 6, 10.1038/ncomms7812, 2015.
559 Apicella, B., Barbella, R., Ciajolo, A., and Tregrossi, A.: Comparative analysis of the structure of carbon
560 materials relevant in combustion, Chemosphere, 51, 1063-1069, http://dx.doi.org/10.1016/S0045-
561 6535(02)00715-4, 2003.
562 Barlow, P. G., Clouter-Baker, A., Donaldson, K., MacCallum, J., and Stone, V.: Carbon black
563 nanoparticles induce type II epithelial cells to release chemotaxins for alveolar macrophages, Part. Fibre
564 Toxicol., 2, 11, 10.1186/1743-8977-2-11, 2005.
565 Baumgartner, J., Zhang, Y., Schauer, J. J., Huang, W., Wang, Y., and Ezzati, M.: Highway proximity and
566 black carbon from cookstoves as a risk factor for higher blood pressure in rural China, Proc. Natl. Acad.
567 Sci. U. S. A., 111, 13229-13234, 10.1073/pnas.1317176111, 2014.
568 Charrier, J. G., and Anastasio, C.: On dithiothreitol (DTT) as a measure of oxidative potential for ambient
569 particles: evidence for the importance of soluble transition metals, Atmos. Chem. Phys., 12, 9321-9333,
570 10.5194/acp-12-9321-2012, 2012.
571 Cho, A. K., Sioutas, C., Miguel, A. H., Kumagai, Y., Schmitz, D. A., Singh, M., Eiguren-Fernandez, A.,
572 and Froines, J. R.: Redox activity of airborne particulate matter at different sites in the Los Angeles Basin,

573 Environmental Research, 99, 40-47, http://dx.doi.org/10.1016/j.envres.2005.01.003, 2005.
574 Fang, T., Verma, V., Bates, J. T., Abrams, J., Klein, M., Strickland, M. J., Sarnat, S. E., Chang, H. H.,
575 Mulholland, J. A., Tolbert, P. E., Russell, A. G., and Weber, R. J.: Oxidative potential of ambient water-
576 soluble PM2.5 in the southeastern United States: contrasts in sources and health associations between
577 ascorbic acid (AA) and dithiothreitol (DTT) assays, Atmos. Chem. Phys., 16, 3865-3879, 10.5194/acp-
578 16-3865-2016, 2016.
579 Hadrup, N., Bengtson, S., Jacobsen, N. R., Jackson, P., Nocun, M., Saber, A. T., Jensen, K. A., Wallin,
580 H., and Vogel, U.: Influence of dispersion medium on nanomaterial-induced pulmonary inflammation
581 and DNA strand breaks: investigation of carbon black, carbon nanotubes and three titanium dioxide
582 nanoparticles, Mutagenesis, 32, 581-597, 10.1093/mutage/gex042, 2017.
583 Han, C., Liu, Y., Liu, C., Ma, J., and He, H.: Influence of Combustion Conditions on Hydrophilic
584 Properties and Microstructure of Flame Soot, J. Phys. Chem. A, 116, 4129-4136, 10.1021/jp301041w,
585 2012a.
586 Han, C., Liu, Y., Ma, J., and He, H.: Effect of soot microstructure on its ozonization reactivity, J. Chem.
587 Phys., 2012 http://dx.doi.org/10.1063/1.4747190, 2012b.
588 He, G., and He, H.: DFT studies on the heterogeneous oxidation of SO2 by oxygen functional groups on
589 graphene, Phys. Chem. Chem. Phys., 18, 31691-31697, 2016.
590 Holder, A. L., Carter, B. J., Goth–Goldstein, R., Lucas, D., and Koshland, C. P.: Increased cytotoxicity
591 of oxidized flame soot, Atmos. Pollu. Res. , 3, 25-31, 2012.
592 Kim, H., Park, K., and Lee, M.-Y.: Biocompatible Dispersion Methods for Carbon Black, Toxicol. Res.,
593 28, 209-216, 2012.
594 Koike, E., and Kobayashi, T.: Chemical and biological oxidative effects of carbon black nanoparticles,
595 Chemosphere, 65, 946-951, http://dx.doi.org/10.1016/j.chemosphere.2006.03.078, 2006.
596 Koromilas, N. D., Lainioti, G. C., Gialeli, C., Barbouri, D., Kouravelou, K. B., Karamanos, N. K.,
597 Voyiatzis, G. A., and Kallitsis, J. K.: Preparation and Toxicological Assessment of Functionalized Carbon
598 Nanotube-Polymer Hybrids, Plos One, 9, 10.1371/journal.pone.0107029, 2014.
599 Kumagai, Y., Koide, S., Taguchi, K., Endo, A., Nakai, Y., Yoshikawa, T., and Shimojo, N. C.: Oxidation
600 of proximal protein sulfhydryls by phenanthraquinone, a component of diesel exhaust particles, Chem.
601 Res. Toxicol., , 15, 483-489, 2002.
602 Kumarathasan, P., Das, D., Salam, M. A., Mohottalage, S., DeSilva, N., Simard, B., and Vincent, R.:
603 Mass spectrometry-based proteomic assessment of the in vitro toxicity of carbon nanotubes, Current
604 Topics in Biochemical Research, 14, 15-27, 2012.
605 Kumarathasan, P., Breznan, D., Das, D., Salam, M. A., Siddiqui, Y., MacKinnon-Roy, C., Guan, J., de
606 Silva, N., Simard, B., and Vincent, R.: Cytotoxicity of carbon nanotube variants: A comparative in vitro
607 exposure study with A549 epithelial and J774 macrophage cells, Nanotoxicology, 9, 148-161,
608 doi:10.3109/17435390.2014.902519, 2014.
609 Kuznetsova, A., Popova, I., Yates, J. T., Bronikowski, M. J., Huffman, C. B., Liu, J., Smalley, R. E., Hwu,
610 H. H., and Chen, J. G.: Oxygen-Containing Functional Groups on Single-Wall Carbon Nanotubes:
611 NEXAFS and Vibrational Spectroscopic Studies, J. Am. Chem. Soc., 123, 10699-10704,
612 10.1021/ja011021b, 2001.
613 Lam, J., Herant, M., Dembo, M., and Heinrich, V.: Baseline Mechanical Characterization of J774
614 Macrophages, Biophysical Journal, 96, 248-254, 2009.
615 Langley, L. A., Villanueva, D. E., and Fairbrother, D. H.: Quantification of Surface Oxides on
616 Carbonaceous Materials, Chem. Mater. , 18, 169-178, 2006.

Lara-Martinez, L. A., Masso, F., Gonzalez, E. P., Garcia-Pelaez, I., Contreras-Ramos, A., Valverde, M., Rojas, E., Cervantes-Sodi, F., and Hernandez-Gutierrez, S.: Evaluating the biological risk of functionalized multiwalled carbon nanotubes and functionalized oxygen-doped multiwalled carbon nanotubes as possible toxic, carcinogenic, and embryotoxic agents, International Journal of Nanomedicine, 12, 7695-7707, 10.2147/ijn.s144777, 2017.

Li, N., Kim, S., Wang, M., Froines, J., Sioutas, C., and Nel, A.: Use of a stratified oxidative stress model to study the biological effects of ambient concentrated and diesel exhaust particulate matter, Inhalation Toxicology, 14, 459-486, 10.1080/089583701753678571, 2002a.

Li, N., Wang, M., Oberley, T. D., Sempf, J. M., and Nel, A. E.: Comparison of the Pro-Oxidative and Proinflammatory Effects of Organic Diesel Exhaust Particle Chemicals in Bronchial Epithelial Cells and Macrophages, J. Immunol., 169, 4531-4541, 2002b.

Li, N., Sioutas, C., Cho, A., Schmitz, D., Misra, C., Sempf, J., Wang, M., Oberley, T., Froines, J., and Nel, A.: Ultrafine particulate pollutants induce oxidative stress and mitochondrial damage, Environmental Health Perspectives, 111, 455-460, 2003.

Li, Q., Wyatt, A., and Kamens, R. M.: Oxidant generation and toxicity enhancement of aged-diesel exhaust, Atmos. Environ., 43, 1037-1042, http://dx.doi.org/10.1016/j.atmosenv.2008.11.018, 2009.

Li, Q., Shang, J., and Zhu, T.: Physicochemical characteristics and toxic effects of ozone-oxidized black carbon particles, Atmos. Environ., 81, 68-75, http://dx.doi.org/10.1016/j.atmosenv.2013.08.043, 2013.

Li, Q., Shang, J., Liu, J., Xu, W., Feng, X., Li, R., and Zhu, T.: Physicochemical characteristics, oxidative capacities and cytotoxicities of sulfate-coated, 1,4-NQ-coated and ozone-aged black carbon particles, Atmos. Res., 153, 535-542, http://dx.doi.org/10.1016/j.atmosres.2014.10.005, 2015.

Li, R. B., Guiney, L. M., Chang, C. H., Mansukhani, N. D., Ji, Z. X., Wang, X., Liao, Y. P., Jiang, W., Sun, B. B., Hersam, M. C., Nel, A. E., and Xia, T.: Surface Oxidation of Graphene Oxide Determines Membrane Damage, Lipid Peroxidation, and Cytotoxicity in Macrophages in a Pulmonary Toxicity Model, ACS Nano, 12, 1390-1402, 10.1021/acsnano.7b07737, 2018.

Liu, Q., Baumgartner, J., Zhang, Y., Liu, Y., Sun, Y., and Zhang, M.: Oxidative Potential and Inflammatory Impacts of Source Apportioned Ambient Air Pollution in Beijing, Environ. Sci. Technol., 48, 12920-12929, 10.1021/es5029876, 2014a.

Liu, Y., Liu, C., Ma, J., Ma, Q., and He, H.: Structural and hygroscopic changes of soot during heterogeneous reaction with O_3, Phys. Chem. Chem. Phys., 12, 10896-10903, 2010.

Liu, Y., Ai, K., and Lu, L.: Polydopamine and Its Derivative Materials: Synthesis and Promising Applications in Energy, Environmental, and Biomedical Fields, Chemical Reviews, 114, 5057-5115, 10.1021/cr400407a, 2014b.

Liu, Y., Liggio, J., Li, S.-M., Breznan, D., Vincent, R., Thomson, E. M., Kumarathasan, P., Das, D., Abbatt, J., Antiñolo, M., and Russell, L.: Chemical and Toxicological Evolution of Carbon Nanotubes During Atmospherically Relevant Aging Processes, Environ. Sci. Technol., 49, 2806-2814, 10.1021/es505298d, 2015.

Long, C. M., Nascarella, M. A., and Valberg, P. A.: Carbon black vs. black carbon and other airborne materials containing elemental carbon: Physical and chemical distinctions, Environmental Pollution, 181, 271-286, http://dx.doi.org/10.1016/j.envpol.2013.06.009, 2013.

M., B. D., K., D., and V., S.: Effects of PM10 in human peripheral blood monocytes and J774 macrophages, Respiratory Research 5, doi:10.1186/1465-9921-5-29, 2004.

Mawhinney, D. B., Naumenko, V., Kuznetsova, A., Yates, J. T., Liu, J., and Smalley, R. E.: Infrared spectral evidence for the etching of carbon nanotubes: Ozone oxidation at 298 K, J. Am. Chem. Soc.,

122, 2383-2384, 10.1021/ja994094s, 2000.

McWhinney, R. D., Badali, K., Liggio, J., Li, S.-M., and Abbatt, J. P. D.: Filterable Redox Cycling Activity: A Comparison between Diesel Exhaust Particles and Secondary Organic Aerosol Constituents, Environ. Sci. Technol., 47, 3362-3369, 10.1021/es304676x, 2013a.

McWhinney, R. D., Zhou, S., and Abbatt, J. P. D.: Naphthalene SOA: redox activity and naphthoquinone gas–particle partitioning, Atmos. Chem. Phys., 13, 9731-9744, 10.5194/acp-13-9731-2013, 2013b.

Muckenhuber, H., and Grothe, H.: The heterogeneous reaction between soot and NO2 at elevated temperature, Carbon 44, 546-559, 2006.

Nel, A., Xia, T., Mädler, L., and Li, N.: Toxic potential of materials at the nanolevel., Science, 311, 622-627, 2006.

Peebles, B. C., Dutta, P. K., Waldman, W. J., Villamena, F. A., Nash, K., Severance, M., and Nagy, A.: Physicochemical and Toxicological Properties of Commercial Carbon Blacks Modified by Reaction with Ozone, Environ. Sci. Technol., 45, 10668-10675, 2011.

Peng, J., Hu, M., Guo, S., Du, Z., Zheng, J., Shang, D., Levy Zamora, M., Zeng, L., Shao, M., Wu, Y.-S., Zheng, J., Wang, Y., Glen, C. R., Collins, D. R., Molina, M. J., and Zhang, R.: Markedly enhanced absorption and direct radiative forcing of black carbon under polluted urban environments, Proc. Natl. Acad. Sci. USA, 113, 4266-4271, 10.1073/pnas.1602310113, 2016.

Schuster, M. E., Hävecker, M., Arrigo, R., Blume, R., Knauer, M., Ivleva, N. P., Su, D. S., Niessner, R., and Schlögl, R.: Surface Sensitive Study To Determine the Reactivity of Soot with the Focus on the European Emission Standards IV and VI, J. Phys. Chem. A., 115, 2568-2580, 10.1021/jp1088417, 2011.

Shvedova, A. A., Pietroiusti, A., Fadeel, B., and Kagan, V. E.: Mechanisms of carbon nanotube-induced toxicity: Focus on oxidative stress, Toxicology and Applied Pharmacology 261, 121-133, 2012.

Simmons, J. M., Nichols, B. M., Baker, S. E., Marcus, M. S., Castellini, O. M., Lee, C. S., Hamers, R. J., and Eriksson, M. A.: Effect of ozone oxidation on single-walled carbon nanotubes, Journal of Physical Chemistry B, 110, 7113-7118, 10.1021/jp0548422, 2006.

Wang, B., Li, K., Jin, W., Lu, Y., Zhang, Y., Shen, G., Wang, R., Shen, H., Li, W., Huang, Y., Zhang, Y., Wang, X., Li, X., Liu, W., Cao, H., and Tao, S.: Properties and Inflammatory Effects of Various Size Fractions of Ambient Particulate Matter from Beijing on A549 and J774A.1 Cells, Environ. Sci. Technol., 47, 10583-10590, 10.1021/es401394g, 2013.

Xia, T., Kovochich, M., Brant, J., Hotze, M., Sempf, J., Oberley, T., Sioutas, C., Yeh, J. I., Wiesner, M. R., and Nel, A. E.: Comparison of the Abilities of Ambient and Manufactured Nanoparticles To Induce Cellular Toxicity According to an Oxidative Stress Paradigm, Nano Letters, 6, 1794-1807, 10.1021/nl061025k, 2006.

Yim, W. L., and Johnson, J. K.: Ozone Oxidation of Single Walled Carbon Nanotubes from Density Functional Theory, Journal of Physical Chemistry C, 113, 17636-17642, 10.1021/jp908089c, 2009.

Zhang, B., Wei, P., Zhou, Z., and Wei, T.: Interactions of graphene with mammalian cells: Molecular mechanisms and biomedical insights, Advanced Drug Delivery Reviews, 105, 145-162, https://doi.org/10.1016/j.addr.2016.08.009, 2016.

Zhang, X., Wang, S., Xu, L., Feng, L., Ji, Y., Tao, L., Li, S., and Wei, Y.: Biocompatible polydopamine fluorescent organic nanoparticles: facile preparation and cell imaging, Nanoscale, 4, 5581-5584, 10.1039/c2nr31281f, 2012.

704 **Figure captions**

705 **Figure 1**. DTT decay rates of several black carbon materials compared with literature
706 results (Li et al., 2013;Charrier and Anastasio, 2012;Liu et al., 2014a;Li et al., 2015;Liu
707 et al., 2015;Holder et al., 2012;Antinolo et al., 2015).

708 **Figure 2**. Cytotoxicity of (A) SB4A, (B) graphene, (C) graphene oxide, (D) SWCNT,
709 (E) SWCNT-OH and (F) SWCNT-COOH toward murine J774 cell line. The stars mean
710 the difference is significant at 0.05 level for a certain dose of carbon nanomaterials
711 compared with the corresponding blank experiments.

712 **Figure 3**. (A) Thermo gravity curves of carbon nanomaterials in nitrogen gas flow;
713 (B) the corresponding differential thermal analysis curves. The insert graph shows the
714 weight loss due to desorption of organics.

715 **Figure 4**. XPS spectra of carbon nanomaterials. (A)-(F) are O1s spectra and (G)-(L)
716 are C1s spectra for SB4A, graphene, graphene oxide, SWCNT, SWCNT-OH and
717 SWCNT-COOH, respectively.

718 **Figure 5**. (A) Distribution of oxygen containing species on the tested carbon
719 nanomaterials; (B) comparison of oxygen-containing species and (C) DTT decay rate
720 between graphene oxide and other carbon nanomaterials.

721 **Figure 6.** DTT decay rate for graphene oxide and thermally treated graphene oxide in N_2 flow
722 at 200 °C.

723

Atmos. Chem. Phys. Discuss., https://doi.org/10.5194/acp-2018-1366
Manuscript under review for journal Atmos. Chem. Phys.
Discussion started: 15 February 2019

Atmospheric Chemistry and Physics Discussions

724 **Figures**

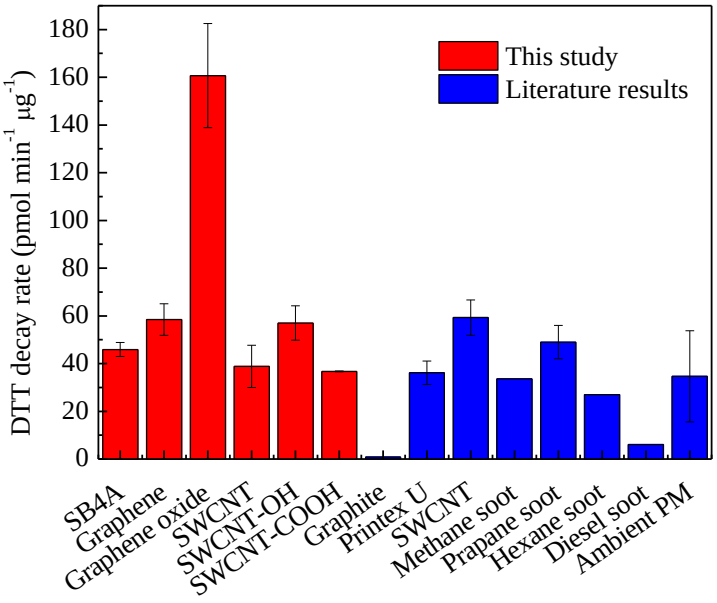

725

726 Fig. 1

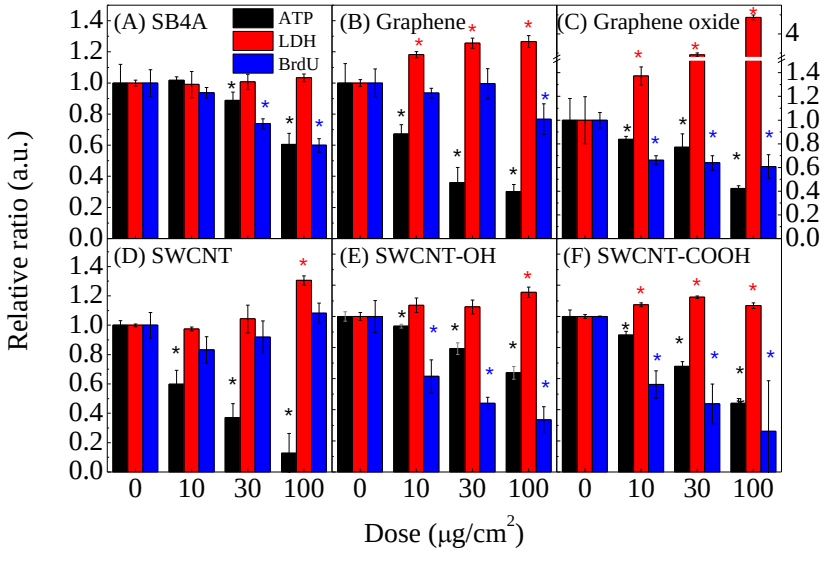

727

728 Fig. 2

Atmos. Chem. Phys. Discuss., https://doi.org/10.5194/acp-2018-1366
Manuscript under review for journal Atmos. Chem. Phys.
Discussion started: 15 February 2019

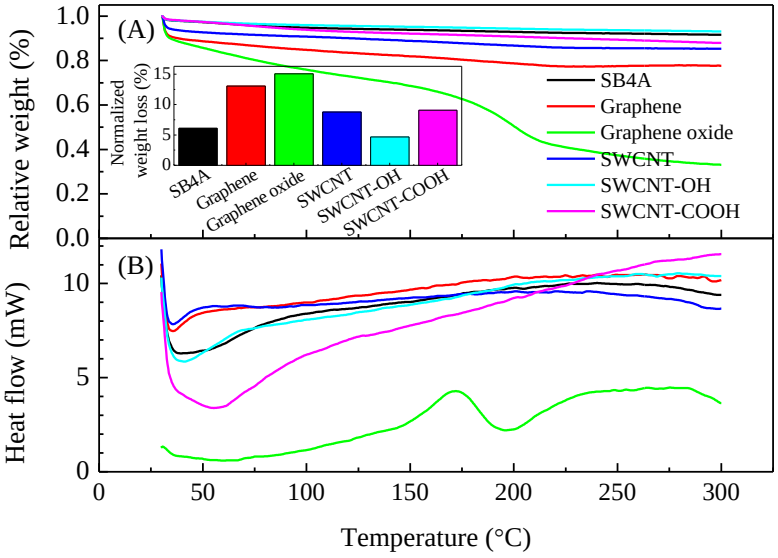

729

730 Fig. 3.

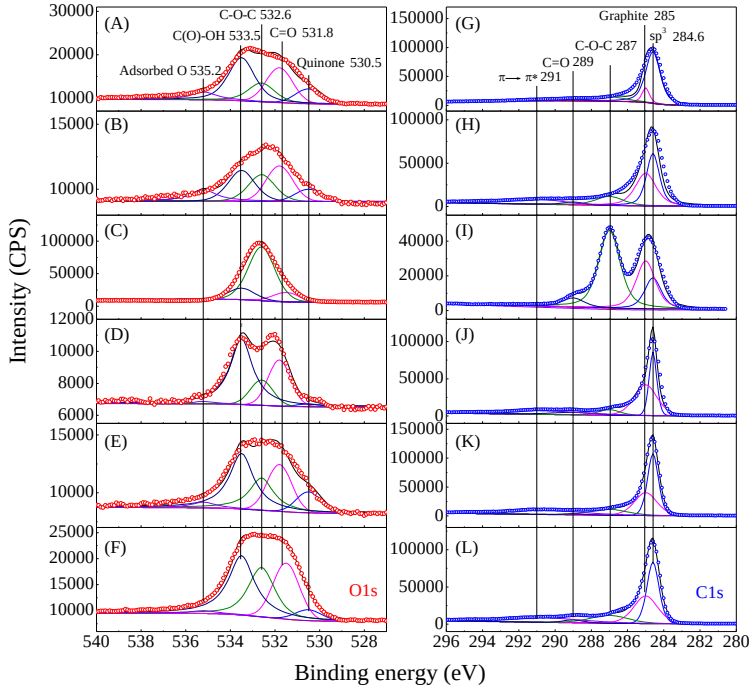

731

Atmos. Chem. Phys. Discuss., https://doi.org/10.5194/acp-2018-1366
Manuscript under review for journal Atmos. Chem. Phys.
Discussion started: 15 February 2019

Atmospheric Chemistry and Physics Discussions

732 Fig. 4.

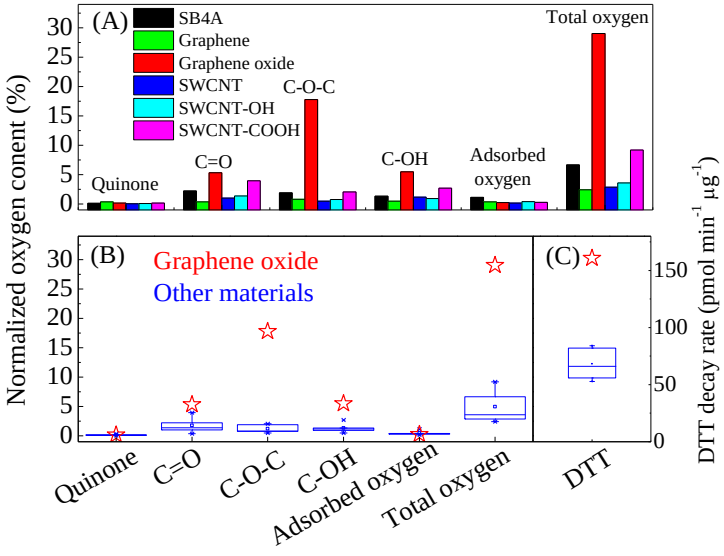

733

734 Fig. 5.

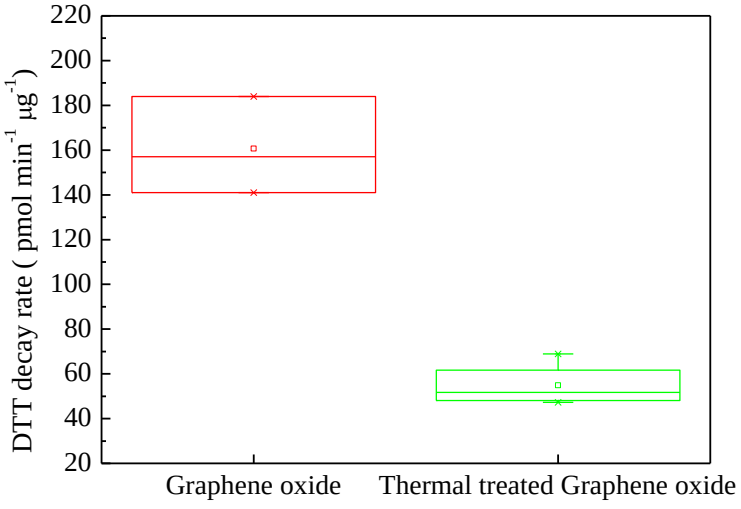

735

736 Figure 6.

737